



ELSEVIER

Contents lists available at [SciVerse ScienceDirect](http://www.sciencedirect.com)

Talanta

journal homepage: www.elsevier.com/locate/talanta

A novel molecularly imprinted impedimetric sensor for melamine determination

Bowan Wu^{a,b}, Zhihua Wang^a, Dongxia Zhao^a, Xiaoquan Lu^{a,*}^a Key Laboratory of Bioelectrochemistry & Environmental Analysis of Gansu Province, College of Chemistry & Chemical Engineering, Northwest Normal University, 730070 Lanzhou, China^b College of Chemistry & Chemical Engineering, Longdong University, 745000 Qingyang, China

ARTICLE INFO

Article history:

Received 12 June 2012

Received in revised form

20 September 2012

Accepted 22 September 2012

Available online 28 September 2012

Keywords:

Electrochemical impedance

Molecularly imprinted

Melamine

2-Mercaptobenzimidazole

ABSTRACT

A novel molecularly imprinted (MIP) impedimetric sensor was promoted for selective detecting melamine (MEL). The Au electrode modified with MIP poly (2-mercaptobenzimidazole) (PMBI) was prepared by electrochemical polymerization of 2-mercaptobenzimidazole (2-MBI) with cyclic voltammetry (CV) in the presence of template molecule MEL. The surface morphology and structure of MIP PMBI are characterized by atomic force microscopy (AFM), infrared spectra (IR), electrochemical impedance spectroscopy (EIS), and CV. The main driving force of recognition is the π -donor–acceptor interaction between MEL and PMBI. The imprinted electrode could avoid the interference successfully. In addition, a linear response curve was obtained from 1.0×10^{-8} M to 5.0×10^{-5} M, with the detection limit of 3.0×10^{-9} M. The sensor exhibits remarkable advantages, such as higher sensitivity, wider linear range and lower detection limit. The effective method has a potential application to monitor nonelectrochemically active substances in food analysis in the future.

© 2012 Elsevier B.V. All rights reserved.

1. Introduction

Melamine (C₃H₆N₆, MEL), a kind of triazine analog with three amino groups, is usually used to produce MEL–formaldehyde resin. In plastics manufacturing, MEL–formaldehyde resins are necessary for making surface coatings, laminates, adhesives, and flame retardants. Due to its high nitrogen level (66% by mass), MEL has been illegally added to dairy products to give a high reading of total nitrogen content as a false measurement of the protein level. In 2007, MEL was found in pet-food products, and led to kidney toxicity in dogs and cats in the USA. In September 2008, the occurrence of kidney stones in thousands of infants across China captured the attention of the world. This situation prompted the US Food and Drug Administration, the European community, and other countries and regions to establish the criteria of maximum residue limits for MEL in various food products. Standard limits of 1 ppm (8 μ M) for MEL in infant formula and 2.5 ppm (20 μ M) in other milk products have been introduced by many countries [1,2]. Investigations of MEL migration in vivo were reported in some literatures [3–5]. Therefore, a sensitive and reliable method is urgently needed for the determination of MEL in food, and is the subject of much recent research, particularly in dairy products for children. Up to now, some

modern instrument analytical methods have been employed for the determination of MEL, such as gas chromatography [6], gas chromatography–mass spectrometry [7], liquid chromatography–mass spectrometry [8], liquid chromatography–triple–quadrupole tandem mass spectrometry [9], high performance liquid chromatography [10], high-performance liquid chromatography–tandem mass spectrometry [11,12], surface enhanced Raman spectroscopy [13], near-infrared/mid-infrared spectroscopy [14], matrix-assisted laser desorption/ionization–mass spectrometry [15], desorption atmospheric pressure chemical ionization mass spectrometry [16], nanoextractive electrospray ionization [17], extractive electrospray ionization mass spectrometry [18], low-temperature plasma probe combined with tandem mass spectrometry [19], nuclear magnetic resonance spectroscopy [20], capillary zone electrophoresis/mass spectrum [21,22], capillary electrophoresis and diode-array detection [23], capillary zone electrophoresis with diode-array detection [24], electrochemiluminescence [25], and chemiluminescence [26]. Unfortunately, the current MEL determination methods, although mostly accurate and sensitive, are difficult to implement for they always require advanced and sophisticated instrumentation, and all the instruments should be operated by some specially trained workers. Moreover, in many instances, they also need a complicated matrix and extensive sample pretreatment including extraction, preconcentration, or derivatization [2,27]. Recently, sensor technology has also been developed for the analysis of MEL and its analogs, including nanoparticle-based sensor [28–31], electrochemical sensor [32–34] and molecularly imprinted polymer

* Corresponding author. Tel: +86 931 7971276; fax: +86 931 7971323.
E-mail address: luxq@nwnu.edu.cn (X. Lu).

(MIP)-based sensor [35–37], because of its sensitivity, rapidity, simplicity and cost effectiveness.

Molecular imprinting technique is an approach to synthesize a polymer matrix with molecular recognition sites, which are specific in shape and size to the target molecule, showing specific high binding behaviors to the target molecules [38]. Due to their mechanical and chemical stabilities, high affinity and outstanding substrate recognition ability, low cost and easy preparation, MIP has been successfully applied in chemical sensing area [39–44]. Different types of electrosynthesized MIP had been reported in the literatures [45–48]. Poly (2-mercaptobenzimidazole) (PMBI) is very stable even under harsh conditions and is widely applied in the field of anti-corrosion [49,50]. The formation and electrosynthesis, characterization and mechanism of PMBI films were previously described in detail [51,52]. 2-mercaptobenzimidazole (2-MBI) contained a mercapto group and might consequently improve the polymer–gold binding characteristics [53–56]. PMBI films seemed suitable for the imprinting procedure because of their compactness, inertness, and high stability derived from the strong adherence to Au.

Electrochemical impedance spectroscopy (EIS) is a powerful tool for examining many chemical and physical processes in solution as well as in solids. EIS has wide applications in corrosion, battery, fuel cell development, sensors and physical electrochemistry and can provide information on reaction parameters, corrosion rates, electrode surfaces porosity, coating, mass transport, and interfacial capacitance measurements [57–59]. In contrast to the numerous MIP-based sensors employing other signal transducing mechanisms reported in literatures, EIS sensors are reported relatively less. In the present study we introduced a novel impedimetric sensor for imprinting of MEL molecular recognition sites that is based on the electropolymerization of 2-MBI on Au electrode. A linear response curve was obtained from 1.0×10^{-8} M to 5.0×10^{-5} M and the detection limit is 3.0×10^{-9} M. Moreover, the interference of some commonly existing substances can be effectively avoided in the detection. The sensor has a wide range for food and feed sample analysis that might be affected by MEL adulteration.

2. Experimental

2.1. Reagents and materials

MEL, glucose and sodium perchlorate (NaClO_4) were purchased from Beijing Chemical Reagent Co. Ltd. Histidine and arginine were purchased from Shanghai Kangda amino acid Factory. 2-mercaptobenzimidazole was purchased from Aladdin Chemistry Co. Ltd. NaOH, absolute ethanol and all other chemicals were of analytical reagent grade and were used as supplied without further purification. All aqueous solutions were prepared with double-distilled water. High-quality nitrogen was used for deaeration.

2.2. Apparatus and equipments

Cyclic voltammetry (CV) and differential pulse voltammetry (DPV) measurements were carried out by a CHI832 electrochemical

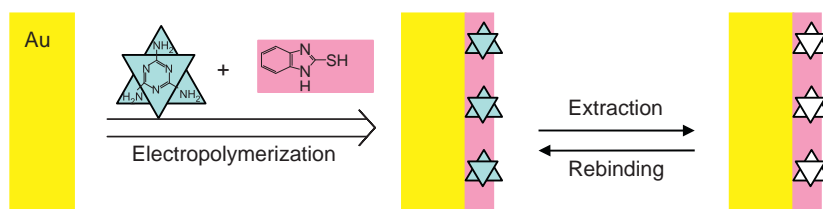
workstation (CHI Instrument Company, Shanghai, China). EIS was conducted on a VMP2 Multi-potentiostat (Princeton Applied Research, USA). A three-electrode system was used in the measurements; bare and modified Au electrode ($d=2$ mm) with a geometrical area (A) of 0.0314 cm^2 each were used as working electrodes. A platinum wire was employed as the counter electrode, and an $\text{Ag}|\text{AgCl}|\text{KCl}$ saturated electrode as the reference electrode. The pH measurements were performed with a PB-10 pH meter (Sartorius, Germany). Atomic force microscopy (AFM) measurements were carried out at ambient temperatures with an Agilent 5400 AFM. The instrument was operated in noncontact (AC) mode using a cantilever with a nominal spring constant of 40 N m^{-1} . The infrared spectra (IR) were measured by a FT-IR spectrometer (Bruker Vertex 70v) under vacuum.

2.3. Preparation of MIP impedimetric sensor

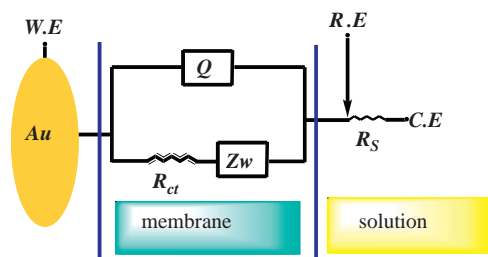
The surface of the Au electrode was polished with 0.3, and 0.05 μm alumina slurry, and also sonicated with double-distilled water after each polishing step. Then the electrodes were cleaned with a 1:3 mixture of 30% H_2O_2 /concentrated H_2SO_4 and rinsed with double-distilled water. Finally the electrode was subjected to cyclic potential sweeps between -0.1 and 0.5 V in 5 mM $[\text{Fe}(\text{CN})_6]^{3-}/[\text{Fe}(\text{CN})_6]^{4-}$ containing 0.1 M KCl as the supporting electrolyte until a stable CV was obtained. The electropolymerization was performed by cyclic voltammetry (10 cycles) in the potential range from -0.1 to 1.3 V with a scan rate of 100 mV s^{-1} . The reaction solution comprises of 80 mM NaClO_4 , 1 mM MEL, 8 mM 2-MBI and ethanol alkaline solution (pH 9.5). Similarly, the nonimprinted electrode was prepared in the same way without addition of the template MEL. The removal of the template MEL was carried out by immersing the electrode prepared above in an ethanol:water (4:1) solution containing 0.1 M NaOH (pH 13) for 20 min at room temperature under continuous agitation. And then it was washed with ethanol and double-distilled water and dried with nitrogen. The finished imprinted electrode was stored at 4°C in dry condition when not in use. A schematic diagram of the sensor preparation is shown in Scheme 1.

2.4. Experimental measurements of MEL

The imprinted electrode was dipped into 3 mL ethanol solution containing the desired concentration of MEL for 5 min, washed with ethanol and double-distilled water carefully to remove the possible adsorptive substances on the electrode surface, and then transferred to the electrochemical cell containing 5 mM $[\text{Fe}(\text{CN})_6]^{3-}/[\text{Fe}(\text{CN})_6]^{4-}$ and 0.1 M KCl as the supporting electrolyte. CV and DPV measurements were performed in the potential range from -0.1 to 0.5 V with a scan rate of 50 mV s^{-1} . The electrochemical cell was connected to a VMP2 Multi-potentiostat interfaced to a PC, which was controlled by EC-Lab (V9.24) software (Bio-Logic SA). EIS was scanned at the formal potential of 0.25 V in the frequency range from 100 kHz to 100 mHz, using an AC voltage of 5 mV amplitude. An $\text{R}(\text{Q}(\text{RW}))$ equivalent circuit could be used to



Scheme 1. Schematic of sensor preparation.



Scheme 2. The equivalent circuit model used to obtain equations for Z_{re} and Z_{im} . W.E is the working electrode, R.E is the reference electrode, and C.E is the counter electrode.

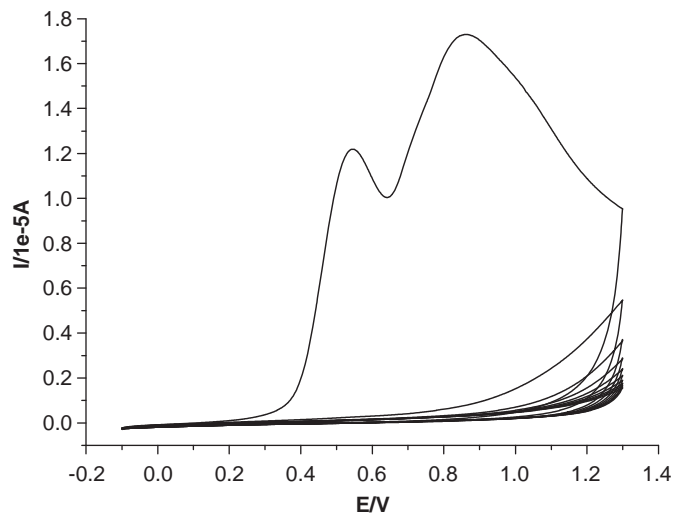


Fig. 1. CV for the electropolymerization MIP in ethanol alkaline solution (pH 9.5) containing 8 mM 2-MBI and 1 mM MEL on Au. Scan rate: 100 mV s^{-1} ; number of scans: 10; potential range: -0.1 to 1.3 V .

simulate the modified Au electrode that was coated with almost nonconductive MIP polymeric film (Scheme 2). The impedance data (R_{ct}) thus obtained were fitted to the $R(Q(RW))$ equivalent circuit using the ZsimpWin (Princeton Applied Research) program. All measurements were performed at room temperature.

3. Results and discussion

3.1. Preparation of polymeric film

A typical CV recorded during electropolymerization in the presence of 2-MBI and MEL is shown in Fig. 1. It was observed that two oxidation peaks appeared during the first cycle and disappeared during the second cycle in the potential range from -0.1 to 1.3 V . The peak current decreased significantly under continuous cyclic scan, indicating that the insulating polymer was formed and bound to the electrode surface. It does not have significant differences in comparison with the CV obtained under the same conditions in the absence of MEL template. The results obtained may contribute to the fact that MEL does not possess electroactivity on gold in the chosen potential range [34] for the polymerization and its structure was not electrochemically altered while the polymer was growing around it.

2-MBI exists in two tautomeric forms, the thioketo and thiolate forms. The thioketo form predominates in acidic solutions, while the thiolate form exists in sufficiently alkaline electrolytes. Therefore, the anodic peaks observed in the first cycle

at 0.546 V and 0.864 V might be assigned to the electrochemical oxidation of the thiol group and pyrrole nitrogen respectively [11,47,49]. The anodic peak at 0.864 V obtained with 2-MBI accounts for the oxidation of the pyrrole nitrogen that allows the building of the polymer network [51].

It is thought that the analyte diffusion into polymer film is slow; an excessively thick layer would not be beneficial for fast response kinetics. Thus, formation of ultrathin polymer films on the electrode surface is preferred to improve the sensitivity of the devices. The thickness of the polymer can be adjusted by controlling the scan rate and the number of cycles during electropolymerization [47]. The film formed on the surface of electrode may be compact and smooth in a slow polymerization process and become rough and porous with the increase in growth rate of films [60,61]. It is known that the molecular template would be entrapped in the polymer firmly and can hardly be removed, because when the scan rate is lower the compact PMBI film will be thicker. However, when the scan rate was too fast, the formed polymerization film would be relatively porous and thin which is not desirable for subsequent use. In order to circumvent the problem, we designed the scan rate relatively high. It was found that the optimized scan rate was 100 mV s^{-1} [46].

The MEL exhibits π -donor properties, thus, the PMBI is the expected electron acceptor. The formation of π -donor-acceptor complexes between MEL and PMBI occurs during the electropolymerization on gold. The optimal position of the π -acceptor sites by subsequent removal of MEL imprint molecules was applied for the association of the MEL analyte.

3.2. AFM evaluation of MEL MIP PMBI morphology

Fig. 2 shows the two-dimensional (left: A1,B1,C1,D1) and three-dimensional (right: A2,B2,C2,D2) AFM images which display surface morphologies of PMBI and MEL copolymer films in different scan ranges (Upper (A and B): scan size $10 \mu\text{m} \times 10 \mu\text{m}$, Down (C and D): scan size $80 \mu\text{m} \times 80 \mu\text{m}$), before (A and C) and after (B and D) remove template molecule. When MEL is removed, the surface of the MIP film becomes rougher and the thickness of imprinted films decreased.

3.3. IR of polymer

The structure studies of the MEL MIP PMBI polymer (MEL-MIP-PMBI) are performed using IR spectroscopy. Fig. 3 shows the IR spectrum of PMBI-MEL extraction (a), PMBI-MEL (b), 2-MBI (c) and MEL (d). For MEL (Fig. 3d), the peaks at 3469 cm^{-1} , 3419 cm^{-1} , and 3333 cm^{-1} represent the vibrating peaks of the $-\text{NH}_2$. For 2-MBI (Fig. 3c), the peak at 3154 cm^{-1} represents the vibrating peak of the N-H. Comparison with curves b, c and d reveals that the peaks become weaker in PMBI (Fig. 3b) because of the interaction between MEL that acts as electron donor and PMBI that acts as electron acceptor. The absorption peaks of triazine ring move from 1652 cm^{-1} , 1552 cm^{-1} , and 1437 cm^{-1} (Fig. 3d) toward 1145 cm^{-1} , 1115 cm^{-1} , and 1089 cm^{-1} respectively in PMBI-MEL film (Fig. 3b). After removing MEL, the peaks of triazine ring almost disappeared (Fig. 3a). The IR absorption peaks of benzene ring around 1465 cm^{-1} decreased (Fig. 3b) because of the interaction between MEL and PMBI. After removing MEL, the peaks of benzene ring increased significantly (Fig. 3a).

3.4. Electrochemical characterization and evaluation of polymeric film

To characterize the different prepared electrodes, CV and DPV were performed with supporting electrolytes containing 5 mM

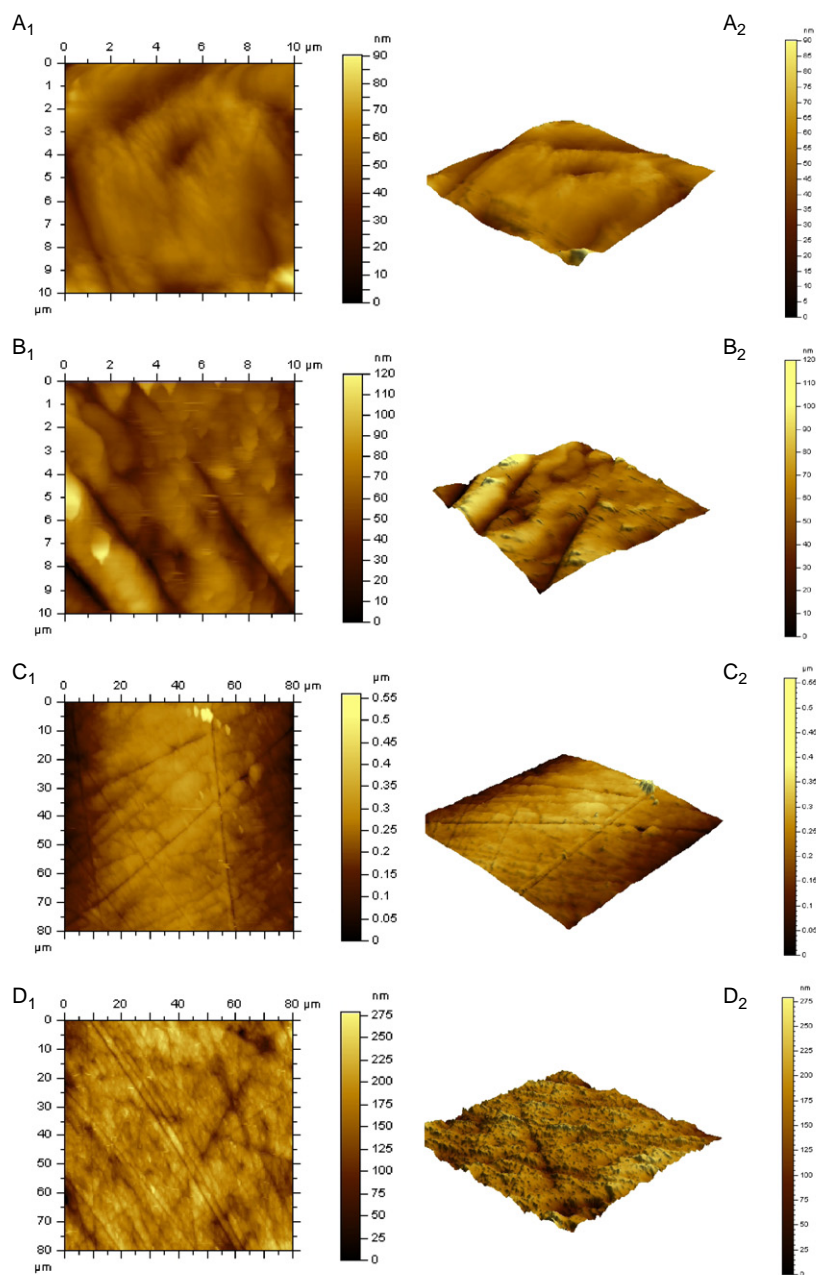


Fig. 2. Two-dimensional (left: A1,B1,C1,D1) and three-dimensional (right: A2,B2,C2,D2) AFM images of PMBI and MEL copolymer films in different scan ranges (Upper (A and B): scan size $10\ \mu\text{m} \times 10\ \mu\text{m}$, Down (C and D): scan size $80\ \mu\text{m} \times 80\ \mu\text{m}$), before (A and C) and after (B and D) remove template molecule.

$[\text{Fe}(\text{CN})_6]^{3-}/[\text{Fe}(\text{CN})_6]^{4-}$ and $0.1\ \text{M}\ \text{KCl}$ in the potential range from -0.1 to $0.5\ \text{V}$ with a scan rate of $50\ \text{mV}\ \text{s}^{-1}$. DPV were recorded with pulse amplitude $50\ \text{mV}$, and pulse width $50\ \text{ms}$. Fig. 4 shows a typical comparison of the CV and DPV among the three types of Au electrode. As we expected, the modification of Au electrode by PMBI film caused a decrease in peak current. It indicates that the electrosynthesized polymer was formed on the surface of Au electrode (shown in Fig. 4(A)b, Fig. 4(B)b).

In fabricating the MIP electrode, MEL was imprinted and formed specific sites on Au electrode by electrosynthesis of PMBI. And the amperometric response of the modified electrode decreased. These results showed that the electron transfer kinetics of $[\text{Fe}(\text{CN})_6]^{3-}/[\text{Fe}(\text{CN})_6]^{4-}$ redox reactions was perturbed when the bare Au electrode was modified with PMBI, confirming that the PMBI was assembled successfully on the gold surface through Au–S bond.

EIS is an effective method for probing the features of a surface modified electrode. In the EIS, the semicircle portion at higher frequencies corresponds to the electron transfer limited process and the linear portion at lower frequencies may ascribe to diffusion. The semicircle diameter equals the electron transfer resistance (R_{ct}) [62], which depends on the dielectric and insulating features at the electrode/electrolyte interface [63–65]. Fig. 5(a) shows the EIS of the bare Au electrode. Almost straight lines were exhibited, which were characteristic of a mass diffusion limiting electron transfer process [66,67]. The results showed faster electron transfer kinetics of $[\text{Fe}(\text{CN})_6]^{3-}/[\text{Fe}(\text{CN})_6]^{4-}$ on the bare Au electrode. After the Au electrode was modified with PMBI in the presence of MEL (Fig. 5(b)), the impedances were significantly enlarged. These results indicate that PMBI membranes have a larger obstruction effect, which leads to reducing electron transfer rate or increasing resistance to the flow of electrons.

When the imprinted PMBI–Au electrode was washed to remove the template molecule (Fig.5(c)), the semicircle diameter was much less than that of the Au electrode modified PMBI with MEL and it was not removed. The reason may be that there were large numbers of the imprinted cavities of MEL in the imprinted PMBI membranes, which enhanced the diffusion rate of $[\text{Fe}(\text{CN})_6]^{3-}/[\text{Fe}(\text{CN})_6]^{4-}$ through the PMBI membranes and made it easier for electron transfer to take place. These results were accordant with AFM and CV assays as described in detail above.

3.5. Analytical performance

In this study, EIS was employed which is relatively sensitive compared with conventional CV and DPV. The responses in the impedance values of the imprinted sensor to 30 μM MEL are shown in Fig. 6. The impedance of the imprinted sensor increased when the imprinted electrode was dipped into 30 μM MEL solution at 5 min. The response time was 5 min, and a steady value was obtained after about 35 min. It was observed that the change of impedance caused by the addition of MEL was reversible and the sensor could be revived by immersion into an ethanol:water (4:1) alkaline solution containing 0.1M NaOH (pH 13) for 20 min.

It is possible that during flash washing of imprinted polymer electrode, some MEL active pores rupture from the electrode. For that reason, the modified electrode will lose its stability after washing 30 times and must be prepared again. However, this phenomenon did not affect electrode performance toward MEL at

low concentration. In fact, in each experiment, relative impedance change is used to determine MEL concentration in the sample solution.

The values of impedance as a function of MEL concentration are plotted in Fig. 7 using the data generated after 5 min of incubation. As at the high concentration range, the impedance tends to be stable, indicating that the imprinting sites were almost occupied by MEL molecules. A linear relationship between impedance and MEL concentration was obtained by covering the concentration in a large range from 1.0×10^{-8} to 5.0×10^{-5} M; the linear regression equation is $R_{ct}(\text{ohm}) = 3248.52 + 1150.421 \text{ g}(\text{C}/\mu\text{M})$, with a correlation coefficient of 0.9979. The detection limit is calculated to be 3×10^{-9} M based on the 3σ of the blank signals.

3.6. The selectivity for MEL detection

In order to assess the impedimetric sensor for the analysis of MEL in dairy products, the interference effects of some substances which were expected to be present in the dairy samples were examined. The solutions used for this purpose contained 20 μM MEL and corresponding interfering species. It showed that, more than 1000-fold excess of NO_3^- , Ac^- , Cl^- , CO_3^{2-} , SO_4^{2-} , PO_4^{3-} , Zn^{2+} , NH_4^+ , Cu^{2+} , Fe^{3+} , Ba^{2+} , Ca^{2+} , Mg^{2+} , Ni^{2+} , Cr^{3+} , Fe^{2+} , and 100-fold excess

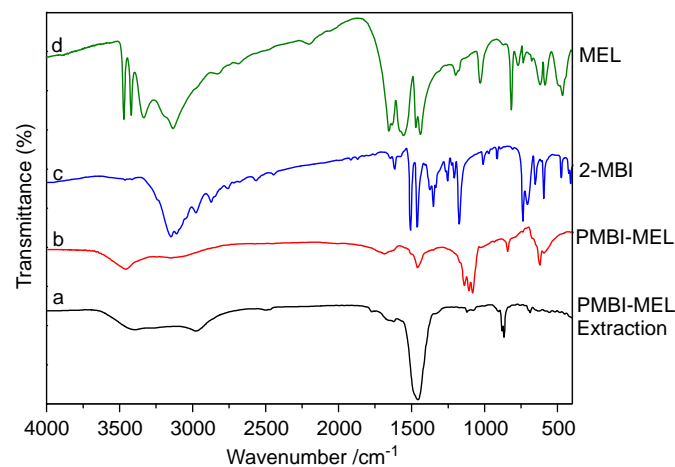


Fig. 3. IR spectrum of PMBI–MEL extraction (a), PMBI–MEL (b), 2-MBI (c) and MEL (d).

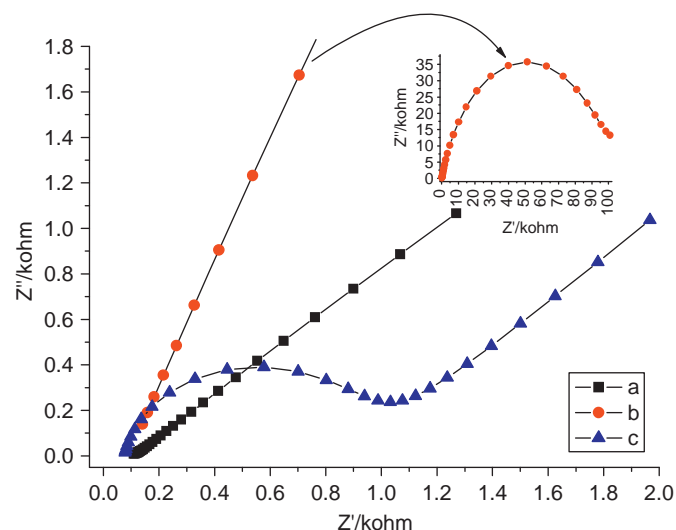


Fig. 5. Complex-plane impedance plots of EIS for 5 mM $[\text{Fe}(\text{CN})_6]^{3-}/[\text{Fe}(\text{CN})_6]^{4-}$ containing 0.1 M KCl at bare Au electrode (a) as well as the Au electrode modified PMBI with MEL (b) before and (c) after MEL was washed. The frequency range is between 100 kHz and 100 mHz with signal amplitude of 5 mV.

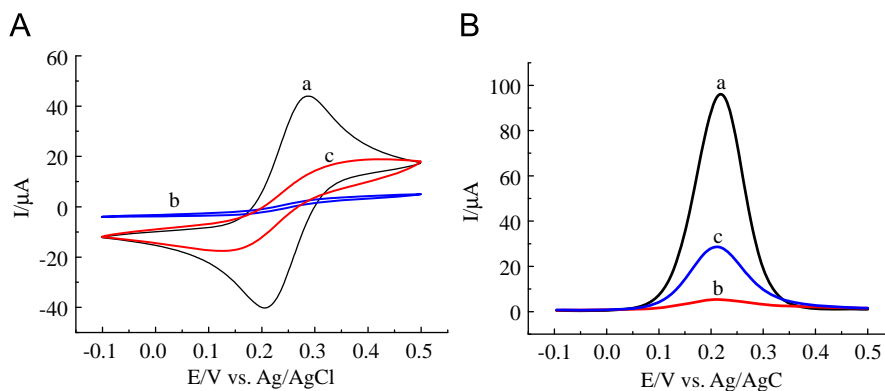


Fig. 4. CV (A) and DPV (B) for different Au electrodes in 5 mM $[\text{Fe}(\text{CN})_6]^{3-}/[\text{Fe}(\text{CN})_6]^{4-}$ containing 0.1 M KCl solution: (a) bare Au electrode; (b) Au electrode modified with PMBI in the presence of MEL; and (c) MIP PMBI modified Au electrode after MEL was washed with alkaline ethanol. Scan rate: 50 mV s^{-1} .

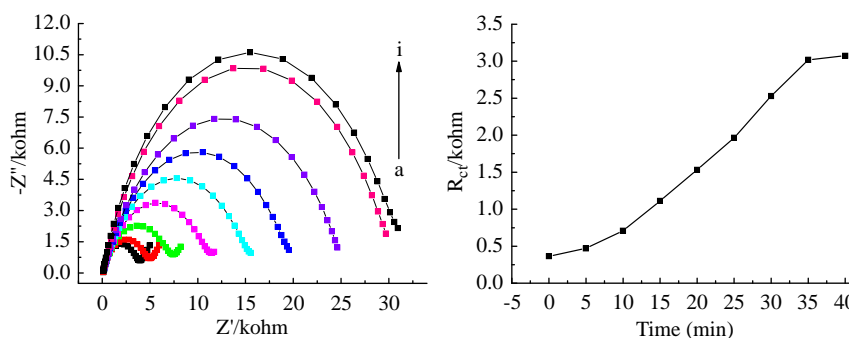


Fig. 6. Impedance response in the presence of 5.0 mM $[\text{Fe}(\text{CN})_6]^{3-}/[\text{Fe}(\text{CN})_6]^{4-}$ containing 0.1 M KCl on imprinted Au after incubation in 30 μM MEL for different times (a–i): 0, 5, 10, 15, 20, 25, 30, 35 and 40 min from bottom to top.

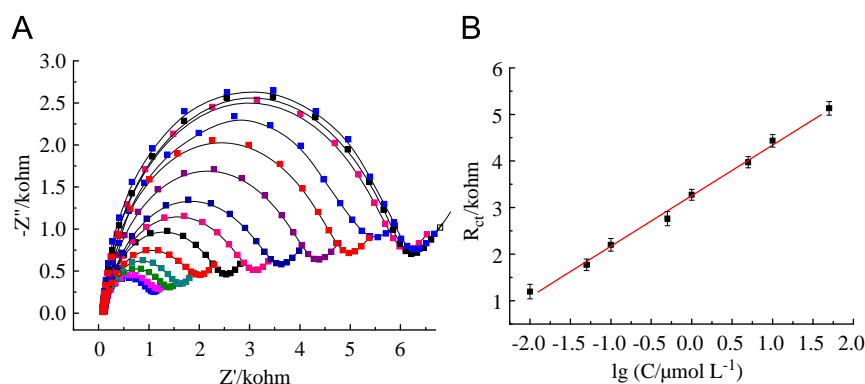


Fig. 7. (A) Impedance response in the presence of 5.0 mM $[\text{Fe}(\text{CN})_6]^{3-}/[\text{Fe}(\text{CN})_6]^{4-}$ containing 0.1 M KCl on imprinted Au after incubation of the electrode for 5 min in various concentrations of MEL: 0, 1.0×10^{-9} , 5.0×10^{-9} , 1.0×10^{-8} , 5.0×10^{-8} , 1.0×10^{-7} , 5.0×10^{-7} , 1.0×10^{-6} , 5.0×10^{-6} , 1.0×10^{-5} , 5.0×10^{-5} , 1.0×10^{-4} , 5.0×10^{-4} and 1.0×10^{-3} M from bottom to top. (B) Calibration curve for MEL.

of fructose, borate, lactose, glucose, urea, lysozyme, uric acid, VB1, VB2, VB6, VC barely interfere in the determination of MEL. The results indicate that the MIP impedimetric sensor exhibits good selectivity toward MEL. In addition, we also analyzed the selectivity pattern of the nonimprinted electrode. An increase in concentrations of MEL did not lead to a significant change in the response. Thus, satisfactory selectivity of MEL was obtained by such a kind of sensor.

3.7. Reproducibility, repeatability and stability

To test the reproducibility of the proposed technique, four MIP impedimetric sensors were constructed under identical experimental conditions. For 30 μM MEL, relative impedance change was obtained by using each of the MIP impedimetric sensors. The standard deviation of the response obtained did not exceed 5%. The repeatability of the sensor was also investigated for 30 μM MEL. The calculated RSD was about 3.8% ($n=8$). The sensor can retain its properties for 3 weeks if stored in air at room temperature. The impedance change upon interaction with 30 μM MEL decreased by about 30% after 1 month of storage. If the sensor is stored in air, the sensors may suffer from contamination which can accumulate over the MEL sites. So it should be stored in a sealed preserving condition at ambient temperature, and washed by ethanol:water (4:1) alkaline solution containing 0.1 M NaOH (pH 13) before use.

3.8. Sample analysis

To assess impedimetric sensors applicability, the proposed method was applied for the analysis of MEL in liquid milk, yogurt and milk powder samples. The concentration of MEL was

Table 1

Determination of MEL in liquid milk, yogurt and milk powder samples.

Sample	Added (μM)	Found (μM)	Recovery (%)	RSD (%) ($n=4$)
Liquid milk	0	0	–	–
	2.5	2.30	92	3.1
	5.0	4.85	97	4.2
	10.0	9.62	96.2	3.0
Yogurt	2.5	2.42	96.8	4.8
	5.0	5.15	103	5.2
	10.0	9.76	97.6	4.3
Milk powder	2.5	2.62	104.8	4.6
	5.0	4.82	96.4	5.3
	10.0	10.12	101.2	4.2

calculated by the standard addition method. The recovery rate of the MIP sensor is less, $\pm 5\%$ (Table 1). Good relative standard deviations (RSDs) of 3.1–5.3% and recoveries of 92–101.2% were obtained. Thus, this proposed method shows potential application for the determination of MEL in dairy products.

To further investigate the performance of the proposed sensor, we compared the results with other methods in Table 2. It can be seen that the sensor exhibits remarkable advantages, such as higher sensitivity, wider linear range and lower detection limit. It is noticed that the recovery obtained in this method provides the requirements for determination of MEL in real samples.

4. Conclusions

A novel electrochemical sensing strategy for sensitive detection of MEL was developed. The new method relies on the π -donor–acceptor interactions between MEL and PMBI. The

Table 2

Comparison of the proposed sensor for MEL detection with other methods.

Methods	Linear range	LOD	Recovery	References
Impedimetric sensor	1.0×10^{-8} – 5.0×10^{-5}	3.0×10^{-9}	92–101.2%	This work
LC-UV and GC-MSD	–	10 ppb	92% and 95%	[6]
DAPCI-MS	10^{-3} –10,000 mg kg ⁻¹	3.4×10^{-15} g mm ⁻²	87–113%	[16]
HPLC	–	5 µg g ⁻¹	81 ± 4%	[10]
Electrochemical sensor	3.9×10^{-8} – 3.3×10^{-6} M	9.6×10^{-9} M	95%	[32]
LC/MS	–	0.008 mg kg ⁻¹	98.9%	[68]
Ion-pair LC-ESI-MS/MS	0.5–100 ng mL ⁻¹	0.01 mg kg ⁻¹	86–89%	[69]
GC-MS and UPLC-MS/MS	1–1000 µg L ⁻¹ and 5–1000 µg L ⁻¹	10 and 5 µg kg ⁻¹	85.2–103.2%	[70]
GC/MS	0.05–2 mg kg ⁻¹	0.01 mg kg ⁻¹	93.9–102%	[71]

imprinted film provided perfect imprinting and impedance performance. The tailor-made cavities formed in the imprinted film showed good selectivity toward MEL. The reproducibility, repeatability and stability of the MIP impedimetric sensor were all found to be satisfactory. The sensing strategy was applied to determine MEL in milk products with satisfying results, which makes great sense in practical detection. In addition, the fabrication procedure was very simple. Compared with other techniques, this method has highly selective separation and enrichment of trace analyte, and has low detection limit down to 3.0×10^{-9} M, which implies that it will have a potential application to monitor nonelectrochemically active substances in complicated real samples in the future.

The new scheme has many advantages for the following reasons: (1) MEL can be absorbed selectively on MIP and the specific binding property greatly improves the selectivity and sensitivity of MEL analysis. (2) When the MEL was reunited in the MIP site, the sensor could be washed with ethanol and double-distilled water carefully to remove the possible adsorptive substances on the electrode surface. (3) The MIP composites system can serve as effective matrices for fast solid phase extraction of the target from analyte samples. (4) Desorption of the analyte at MIP composites can be readily revived by ethanol:water (4:1) alkaline solution containing 0.1 M NaOH (pH 13). (5) It is possible that both extraction and EIS detection can be carried out at the same MIP composites.

Acknowledgments

This work is supported by the National Natural Science Foundation of China (Nos. 20965007, 21175108, 21165016, 21005063, 21165015, 20927004), the Science and Technology Support Projects of Gansu Province (No.1011GKCA025), the Natural Science Foundation of Gansu Province (Nos.096RJZA121 and 096RJZA122), Key Laboratory of Eco-Environment-Related Polymer Materials, Ministry of Education of China, and Key Laboratory of Gansu Polymer Materials.

References

- [1] C.-W. Kim, J.-W. Yun, I.-H. Bae, J.-S. Lee, H.-J. Kang, K.-M. Joo, H.-J. Jeong, J.-H. Chung, Y.-H. Park, K.-M. Lim, *Chem. Res. Toxicol.* 23 (2009) 220–227.
- [2] F. Sun, W. Ma, L. Xu, Y. Zhu, L. Liu, C. Peng, L. Wang, H. Kuang, C. Xu, *Trends Anal. Chem.* 29 (2010) 1239–1249.
- [3] Z. Chik, D.E.M. Haron, E.D. Ahmad, H. Taha, A.M. Mustafa, *Food Addit. Contam. A* 28 (2011) 967–973.
- [4] X.F. Dong, S.Y. Liu, J.M. Tong, Q. Zhang, *Food Addit. Contam. A* 27 (2010) 1372–1379.
- [5] I.J. Wang, C.C. Chen, C.C. Chan, P.C. Chen, G. Leonardi, K.Y. Wu, *Food Addit. Contam. A* 28 (2011) 384–395.
- [6] R.A. Yokley, L.C. Mayer, R. Rezaaiyan, M.E. Manuli, M.W. Cheung, *J. Agric. Food Chem.* 48 (2000) 3352–3358.
- [7] X. Zhu, S. Wang, Q. Liu, Q. Xu, S. Xu, H. Chen, *J. Agric. Food Chem.* 57 (2009) 11075–11080.
- [8] W.C. Andersen, S.B. Turnipseed, C.M. Karbiwnyk, S.B. Clark, M.R. Madson, C.M. Gieseker, R.A. Miller, N.G. Rummel, R. Reimschuessel, *J. Agric. Food Chem.* 56 (2008) 4340–4347.
- [9] S.A. Tittlemier, B.P.Y. Lau, C. Me'nard, C. Corrigan, M. Sparling, D. Gaertner, K. Pepper, M. Feeley, *J. Agric. Food Chem.* 57 (2009) 5340–5344.
- [10] S. Ehling, S. Tefera, I.P. Ho, *Food Addit. Contam.* 24 (2007) 1319–1325.
- [11] M.S. Filigenzi, E.R. Tor, R.H. Poppenga, L.A. Aston, B. Puschner, *Rapid Commun. Mass Spectrom.* 21 (2007) 4027–4032.
- [12] M.S. Filigenzi, B. Puschner, L.S. Aston, R.H. Poppenga, *J. Agric. Food Chem.* 56 (2008) 7593–7599.
- [13] M. Lin, L. He, J. Awika, L. Yang, D.R. Ledoux, H. Li, A. Mustapha, *J. Food Sci.* 73 (2008) T129–T134.
- [14] L.J. Mauer, A.A. Chernyshova, A. Hiatt, A. Deering, R. Davis, *J. Agric. Food Chem.* 57 (2009) 3974–3980.
- [15] H.-W. Tang, K.-M. Ng, S.S.-Y. Chui, C.-M. Che, C.-W. Lam, K.-Y. Yuen, T.-S. Siu, L.C.-L. Lan, X. Che, *Anal. Chem.* 81 (2009) 3676–3682.
- [16] S. Yang, J. Ding, J. Zheng, B. Hu, J. Li, H. Chen, Z. Zhou, X. Qiao, *Anal. Chem.* 81 (2009) 2426–2436.
- [17] M. Li, B. Hu, J. Li, R. Chen, X. Zhang, H. Chen, *Anal. Chem.* 81 (2009) 7724–7731.
- [18] L. Zhu, G. Gamez, H. Chen, K. Chinglin, R. Zenobi, *Chem. Commun.* (2009) 559–561.
- [19] G. Huang, Z. Ouyang, R.G. Cooks, *Chem. Commun.* (2009) 556–558.
- [20] D.W. Lachenmeier, E. Humpfer, F. Fang, B. Schutz, P. Dvortsak, C. Sproll, M. Spraul, *J. Agric. Food Chem.* 57 (2009) 7194–7199.
- [21] H.A. Cook, C.W. Klampfl, W. Buchberger, *Electrophoresis* 26 (2005) 1576–1583.
- [22] C.W. Klampfl, L. Andersen, M. Haunschmidt, M. Himmelsbach, W. Buchberger, *Electrophoresis* 30 (2009) 1743–1746.
- [23] Z. Chen, X. Yan, *J. Agric. Food Chem.* 57 (2009) 8742–8747.
- [24] N. Yan, L. Zhou, Z. Zhu, X. Chen, *J. Agric. Food Chem.* 57 (2009) 807–811.
- [25] Z. Guo, P. Gai, T. Hao, S. Wang, D. Wei, N. Gan, *Talanta* 83 (2011) 1736–1741.
- [26] Z. Wang, D. Chen, X. Gao, Z. Song, *J. Agric. Food Chem.* 57 (2009) 3464–3469.
- [27] S.A. Tittlemier, *Food Addit. Contam. A* 27 (2010) 129–145.
- [28] L. Li, B. Li, D. Cheng, L. Mao, *Food Chem.* 122 (2010) 895–900.
- [29] H. Chi, B. Liu, G. Guan, Z. Zhang, M.-Y. Han, *Analyst* 135 (2010) 1070–1075.
- [30] C. Han, H. Li, *Analyst* 135 (2010) 583–588.
- [31] K. Ai, Y. Liu, L. Lu, *J. Am. Chem. Soc.* 131 (2009) 9496–9497.
- [32] Q. Cao, H. Zhao, L. Zeng, J. Wang, R. Wang, X. Qiu, Y. He, *Talanta* 80 (2009) 484–488.
- [33] Q. Cao, H. Zhao, Y. He, N. Ding, J. Wang, *Anal. Chim. Acta* 675 (2010) 24–28.
- [34] H. Zhu, S. Zhang, M. Li, Y. Shao, Z. Zhu, *Chem. Commun.* 46 (2010) 2259–2261.
- [35] A. Pietrzyk, W. Kutner, R. Chitta, M.E. Zandler, F. D'Souza, F. Sannicola, P.R. Mussini, *Anal. Chem.* 81 (2009) 10061–10070.
- [36] Y.T. Liu, J. Deng, X.L. Xiao, L. Ding, Y.L. Yuan, H. Li, X.T. Li, X.N. Yan, L.L. Wang, *Electrochim. Acta* 56 (2011) 4595–4602.
- [37] R. Liang, R. Zhang, W. Qin, *Sens. Actuators B* 141 (2009) 544–550.
- [38] Z. Wang, H. Li, J. Chen, Z. Xue, B. Wu, X. Lu, *Talanta* 85 (2011) 1672–1679.
- [39] K.D. Shimizu, C.J. Stephenson, *Curr. Opin. Chem. Biol.* 14 (2010) 743–750.
- [40] L. Chen, S. Xu, J. Li, *Chem. Soc. Rev.* 40 (2011) 2922–2942.
- [41] E. Turiel, A. Martín-Esteban, *Anal. Chim. Acta* 668 (2010) 87–99.
- [42] V. Suryanarayanan, C.-T. Wu, K.-C. Ho, *Electroanalysis* 22 (2010) 1795–1811.
- [43] K. Haupt, *Analyst* 126 (2001) 747–756.
- [44] H.-H. Yang, W.-H. Zhou, X.-C. Guo, F.-R. Chen, H.-Q. Zhao, L.-M. Lin, X.-R. Wang, *Talanta* 80 (2009) 821–825.
- [45] K. Haupt, K. Mosbach, *Chem. Rev.* 100 (2000) 2495–2504.
- [46] J.L. Gong, F.C. Gong, G.M. Zeng, G.L. Shen, R.Q. Yu, *Talanta* 61 (2003) 447–453.
- [47] A. Aghaei, M.R. Milani Hosseini, M. Najafi, *Electrochim. Acta* 55 (2010) 1503–1508.
- [48] L. Feng, Y. Liu, Y. Tan, J. Hu, *Biosens. Bioelectron.* 19 (2004) 1513–1519.
- [49] G. Xue, X.-Y. Huang, J. Dong, J. Zhang, *J. Electroanal. Chem.* 310 (1991) 139–148.
- [50] M. Benmessaoud, K. Es-salah, N. Hajjaji, H. Takenouti, A. Srhiri, M. Ebentouhami, *Corros. Sci.* 49 (2007) 3880–3888.
- [51] F.X. Perrin, J. Pagetti, *Corros. Sci.* 40 (1998) 1647–1662.
- [52] B. Assouli, Z.A. Ait Chikh, H. Idrissi, A. Srhiri, *Polymer* 42 (2001) 2449–2454.
- [53] W.A. Hayes, H. Kim, X. Yue, S.S. Perry, C. Shannon, *Langmuir* 13 (1997) 2511–2518.

- [54] T. Doneux, F. Tielens, P. Geerlings, C. Buess-Herman, J. Phys. Chem. A 110 (2006) 11346–11352.
- [55] T. Doneux, C. Buess-Herman, M.G. Hosseini, R.J. Nichols, J. Lipkowski, Electrochim. Acta 50 (2005) 4275–4282.
- [56] T. Doneux, C. Buess-Herman, J. Lipkowski, J. Electroanal. Chem. 564 (2004) 65–75.
- [57] O.A. Loaiza, P.J. Lamas-Ardisana, E. Jubete, E. Ochoteco, I. Loinaz, G.n. Cabanero, I. Garcí'a, S. Penades, Anal. Chem. 83 (2011) 2987–2995.
- [58] R. Thoelen, R. Vansweevelt, J. Duchateau, F. Horemans, J. D'Haen, L. Lutsen, D. Vanderzande, M. Ameloot, M. vandeVen, T.J. Cleij, P. Wagner, Biosens. Bioelectron. 23 (2008) 913–918.
- [59] W.M. Hassen, C. Chaix, A. Abdelghani, F. Bessueille, D. Leonard, N. Jaffrezic-Renault, Sens. Actuators B 134 (2008) 755–760.
- [60] T. Osaka, K. Naoi, S. Ogano, S. Nakamura, J. Electrochem. Soc. 134 (1987) 2096–2102.
- [61] K. Kanamura, Y. Kawai, S. Yonezawa, Z. Takehara, J. Phys. Chem. 98 (1994) 2174–2179.
- [62] J. Zhang, Y. Wang, R. Lv, L. Xu, Electrochim. Acta 55 (2010) 4039–4044.
- [63] J. Li, J. Zhao, X. Wei, Sens. Actuators B 140 (2009) 663–669.
- [64] P. Solanki, N. Prabhakar, M. Pandey, B. Malhotra, Biomed. Microdevices 10 (2008) 757–767.
- [65] L.-P. Lu, S.-Q. Wang, X.-Q. Lin, Anal. Chim. Acta 519 (2004) 161–166.
- [66] Y. Liu, Y. Yu, Q. Yang, Y. Qu, Y. Liu, G. Shi, L. Jin, Sens. Actuators B 131 (2008) 432–438.
- [67] G. Jie, B. Liu, H. Pan, J.-J. Zhu, H.-Y. Chen, Anal. Chem. 79 (2007) 5574–5581.
- [68] E. Braekevelt, B.P.Y. Lau, S. Feng, C. Ménard, S.A. Tittlemier, Food Addit. Contam. A 28 (2011) 698–704.
- [69] J.V. Sancho, M. Ibáñez, S. Grimalt, Ó.J. Pozo, F. Hernández, Anal. Chim. Acta 530 (2005) 237–243.
- [70] X. Xia, S. Ding, X. Li, X. Gong, S. Zhang, H. Jiang, J. Li, J. Shen, Anal. Chim. Acta 651 (2009) 196–200.
- [71] X.-m. Xu, Y.-p. Ren, Y. Zhu, Z.-x. Cai, J.-l. Han, B.-f. Huang, Y. Zhu, Anal. Chim. Acta 650 (2009) 39–43.